1-1-2011

An analytical simulation technique for cone-beam CT and pinhole SPECT

Xuezhu Zhang
Chinese Academy Of Sciences

Yujin Qi
University of Wollongong, yujin@uow.edu.au

An analytical simulation technique for cone-beam CT and pinhole SPECT

Abstract

This study was aimed at developing an eficient simulation technique with an ordinary PC ﹒ The work involved derivation of mathematical operators ﹐ analytic phantom generations ﹐ and effective analytical projectors developing for cone—beam CT and pinhole SPECT imaging ﹒ The computer simulations based on the analytical projectors were developed by ray—tracing method for cone—beam CT and voxel—driven method for pinhole SPECT of degrading blurring ﹒ The 3D Shepp Logan ﹐ Jaszczak and Defrise phantoms were used for simulation evaluations and image reconstructions ﹒ The reconstructed phantom images were of good accuracy with the phantoms ﹒ The results showed that the analytical simulation technique is an efı cient tool for studying cone—beam CT and pinhole SPECT im aging ﹒

Keywords

spect, pinhole, ct, analytical, beam, simulation, technique, cone

Disciplines

Engineering | Science and Technology Studies

Publication Details

Zhang, X. & Qi, Y. (2011). An analytical simulation technique for cone-beam CT and pinhole SPECT. Nuclear Science and Techniques, 22 (6), 338-343.

An analytical simulation technique for cone-beam CT and pinhole SPECT imaging

ZHANG Xuezhu, QI Yujin*

Shanghai Institute of Applied Physics, *Chinese Academy of Sciences*, *Shanghai 201800*, *China*

Abstract This study was to develop an efficient computer simulation technique in the general PC, involving in derivation of mathematical operators, analytic phantom generations, and development of effective analytical projectors for the cone-beam CT and pinhole SPECT imaging. The computer simulations based on the derived analytical projectors were developed using ray-tracing method for Cone-beam CT and voxel-driven method for pinhole SPECT with degrading blurring. The 3D Shepp-Logan phantom, Jaszczak phantom and Defrise phantom were used for the simulation evaluations and image reconstructions. The reconstructed phantom images showed a good accuracy with the phantoms. The results showed that our analytical simulation technique is an efficient tool for studying cone-beam CT and pinhole SPECT imaging.

Key words Computer simulation, Mathematical Phantom, Cone-beam CT, Pinhole SPECT

1 Introduction

Computer simulation has been widely used in the scientific research, product development and practical predictive applications[1–2]. In the study of medical imaging, especially the radiology and nuclear medicine imaging, computer simulation plays an important role in the validation and implementation of various image reconstruction methods, design of objective imaging system, evaluation of image quality, etc[3–4]. Along with the emerging pre-clinical molecular imaging techniques such as X-ray computed tomography (Micro-CT) and single photon emission computed tomography (Micro-SPECT) for *in vivo* small animal imaging, computer simulations are utilized to investigate high performance instrumentation before developing practical imaging systems.

To achieve quantitative accuracy with the real imaging systems, the statistical simulation methods such as the Monte Carlo (MC) simulation are usually required. However, MC simulations need massive computations which are extremely time-consuming and cost expensive. If there is neither a sufficient high performance computer nor parallel computer cluster, the computation tasks using MC methods are not practical and applicable. In this study, we aimed to develop an effective analytical computer simulation technique which is applicable in the general PC for both cone-beam CT and pinhole SPECT imaging. The mathematical derivation of imaging formation was investigated first with analytical coordinate transformation and projection operation. The adaptive mathematical phantoms were designed and implemented for different imaging modalities and acquisition modes. The performances of our developed analytical computer simulation techniques were evaluated and validated using phantom computational experiments and corresponding image reconstruction for cone-beam CT, single-pinhole SPECT with circular -orbit and helical-orbit scan modes and multi- pinhole SPECT imaging.

2 Methods and materials

2.1 General image formation modeling

The principles of X-ray CT imaging could be briefly depicted as low energy photons radiated from the X- ray tube, penetrated through the object, and detected by the X-ray detector. Similarly, SPECT are the gamma photons emitted from the concentrated radioactive tracer in vivo, passed through the object and the collimator, and detected by the gamma camera [5–7]. The image formation of the both imaging modalities could be approximately described by the mathematical methods as the continuous integral model, and briefly formulated as Eq.(1) by a series of derivation without considering the degrading factors such as attenuation, scatter, and noise effects.

$$P = \int_L f(\boldsymbol{x})\,\mathrm{d}\boldsymbol{x} \qquad (1)$$

For the calculation of integral, a term nominated as ray-tracing is regularly taken in image reconstruction and computer simulation. This method describes that the radiation ray transmits the object and their intersection are the tracing integral portion, which the projection of the radial beam.

Also, the mathematical methods of image formation could be approximately described as discrete projection equations, in which the imaging object is visualized as voxellated matrix. Eq.(2) is a brief discretized model for the

*Corresponding author (email: qiyujin@sinap.ac.cn)

This work was supported in part by National Natural Science Foundation of China (Grant No. 10875162)

projection procedure.

$$P = \sum_{j=1}^{M} C_j \bar{f}(\boldsymbol{x}) \qquad (2)$$

At this moment, a method named voxel-driven depicts that the projection is the summation of photons about the transmission attenuation coefficient of CT or the emission radioactivity of SPECT from the voxels of imaging object to the detector bins.

The inverse problems about image reconstruction from projections are the primary issues for CT and SPECT imaging. The ray-tracing and the voxel-driven methods, which are the kernel conceptions and approaches in the mathematical theory and computer processing, will be used for the practical implementation of both image reconstruction and computer simulation about the cone-beam CT and pinhole SPECT imaging in our study.

2.2 Projection operators of cone-beam CT and pinhole SPECT

The mathematical modelling of image formation and reconstruction for CT and SPECT refers to the coordinate transformation in specific imaging geometry. We assume that the object rotates around the axis of rotation (AOR) and the detector is stationary. The coordinate transformation about cone-beam CT and pinhole SPECT imaging can be derived as the projection operators in Cartesian coordinate systems[8–9]. Fig.1 shows the schematics about the coordinate transformation from the object reference system ($O'''x'''y'''z'''$) to the detector imaging reference system ($Oxyz$), which relates to three angle rotation: one angle rotation θ around the AOR, one tilted angle rotation (α) from $O'''x'''$ to Ox, one screwed angle rotation (β) from $O'''y'''$ to Oy, and one coordinate translation (x_c, y_c, z_c). These can be described as Eq.(3), which are the four times multiplication of the operators $\boldsymbol{R}_\theta$, $\boldsymbol{R}_\alpha$, $\boldsymbol{R}_\beta$ and $\boldsymbol{T}$, and α, β and θ are all assumed as clock-wise angle.

The coordinate of the focal center of X-ray tube (FC) or pinhole collimator (PH) is (x_p, y_p, z_p), in which $x_p > x_c$ for cone-beam CT and $x_p < x_c$ for pinhole SPECT. The projection operators of cone-beam and pinhole imaging are derived and presented in Eq.(4), in which (x_d, y_d, z_d) denotes the projection coordinate of the object transmitted by X-ray source or emitted through pinhole collimator to the detector plane where $x_d = 0$.

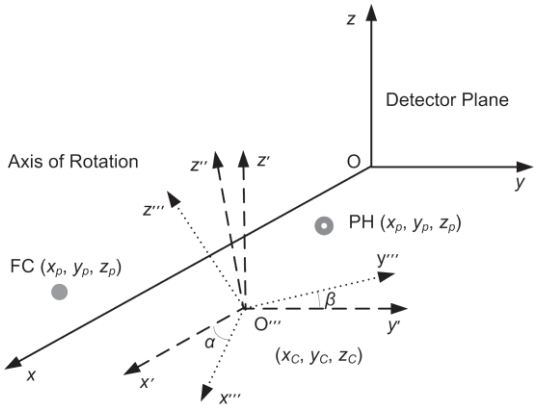

Fig.1 Schematics of the coordinate transformation from the object reference system to the detector imaging reference system for both the cone-beam CT and pinhole SPECT imaging.

$$\boldsymbol{R}_\theta = \begin{bmatrix} \cos\theta & \sin\theta & 0 & 0 \\ -\sin\theta & \cos\theta & 0 & 0 \\ 0 & 0 & 1 & 0 \\ 0 & 0 & 0 & 1 \end{bmatrix}, \quad \boldsymbol{R}_a = \begin{bmatrix} \cos\alpha & 0 & \sin\alpha & 0 \\ 0 & 1 & 0 & 0 \\ -\sin\alpha & 0 & \cos\alpha & 0 \\ 0 & 0 & 0 & 1 \end{bmatrix}$$

$$\boldsymbol{R}_\beta = \begin{bmatrix} 1 & 0 & 0 & 0 \\ 0 & \cos\beta & -\sin\beta & 0 \\ 0 & \sin\beta & \cos\beta & 0 \\ 0 & 0 & 0 & 1 \end{bmatrix}, \quad \boldsymbol{T} = \begin{bmatrix} 1 & 0 & 0 & x_c \\ 0 & 1 & 0 & y_c \\ 0 & 0 & 1 & z_c \\ 0 & 0 & 0 & 1 \end{bmatrix}$$

$$\begin{bmatrix} x_\theta & y_\theta & z_\theta & 1 \end{bmatrix}^T = \boldsymbol{T} \times \boldsymbol{R}_\beta \times \boldsymbol{R}_\alpha \times \boldsymbol{R}_\theta \times \begin{bmatrix} x''' & y''' & z''' & 1 \end{bmatrix}^T \quad (3)$$

$$y_d = y + \left(\frac{x_d - x}{x - x_p} \right)\left(y - y_p \right),\ z_d = z + \left(\frac{x_d - x}{x - x_p} \right)\left(z - z_p \right) \quad (4)$$

In the following discussion, we will implement the computer simulation and image reconstruction of cone-beam CT and pinhole SPECT imaging based on the above reference framework of the coordinate transformation.

2.3 Analytical phantom generations

The mathematical phantoms for computer simulation of radiological imaging can be divided into analytical phantom and anthropomorphic phantom which involve stylized modals and voxel-based modals[10]. Similar to MC methods, the anthropomorphic simulations are extremely computational consuming in which the general PCs cannot undertake the practical computation tasks. Based on geometrical model such as ellipsoid or cylinder, the analytical phantoms are very simple and can be easily implemented for general computational condition. For our imaging studies, we developed several analytical phantoms including 3D Shepp-Logan phantom, Hot-Spot phantom and Defrise phantom which are used as the routine evaluation tools in the computer simulation of CT and SPECT.

3D Shepp-Logan phantom are based on ellipsoids with different size which is extensively used in the early CT study to approximately simulate the tissue of human's head[11]. It belongs to ellipsoid phantom and could be described as analytical second-order quadratic equation formulated as Eq.(5), in which (u''', v''', and w''') are the coordinate in the object reference system ($O'''x'''y'''z'''$) introduced in Section 1.2, (u'''_c, v'''_c, and w'''_c) are the center position of a specific ellipsoid, a, b, and c are the three corresponding axial radius.

$$\left(\frac{u''' - u'''_c}{a} \right)^2 + \left(\frac{v''' - v'''_c}{b} \right)^2 + \left(\frac{w''' - w'''_c}{c} \right)^2 \le 1 \quad (5)$$

3D Hot-Spot Jaszczak phantom is based on hollow cylinders with different diameter channels, and widely used for the SPECT studies to evaluate the reconstruction resolution of the imaging system. Also, 3D Defrise phantom consisted of flat cylinders is used to evaluate the axial imaging resolution. Both of them are cylinder phantom and can be described as Eq.(6), the coordinate of the height position (w) of the cylinder must be constrained in the region $[-w'''_{\min}, w'''_{\max}]$ in which $-w'''_{\min}$ and $w'''_{\max}$ are the coordinate of the bottom and the top surfaces respectively.

$$\left(\frac{u''' - u'''_c}{a} \right)^2 + \left(\frac{v''' - v'''_c}{b} \right)^2 \le 1,\ -w'''_{\min} \le w \le w'''_{\max} \quad (6)$$

The geometrical modal may be position at any direction, so a given position of the phantom in the object reference system $O'''x'''y'''z'''$ relates to another coordinate transformation similar to the derivation of section 1.2. Also, it can be described as the multiplication of the operators (M'''_φ, M''', M'''_η and T''') (Eq. (7)).

$$\boldsymbol{M}'''_\phi = \begin{bmatrix} \cos\phi & \sin\phi & 0 & 0 \\ -\sin\phi & \cos\phi & 0 & 0 \\ 0 & 0 & 1 & 0 \\ 0 & 0 & 0 & 1 \end{bmatrix},\quad \boldsymbol{M}'''_\rho = \begin{bmatrix} \cos\rho & 0 & \sin\rho & 0 \\ 0 & 1 & 0 & 0 \\ -\sin\rho & 0 & \cos\rho & 0 \\ 0 & 0 & 0 & 1 \end{bmatrix}$$

$$\boldsymbol{M}'''_\eta = \begin{bmatrix} 1 & 0 & 0 & 0 \\ 0 & \cos\eta & -\sin\eta & 0 \\ 0 & \sin\eta & \cos\eta & 0 \\ 0 & 0 & 0 & 1 \end{bmatrix},\quad \boldsymbol{T}''' = \begin{bmatrix} 1 & 0 & 0 & u'''_c \\ 0 & 1 & 0 & v'''_c \\ 0 & 0 & 1 & w'''_c \\ 0 & 0 & 0 & 1 \end{bmatrix}$$

$$\begin{bmatrix} x''' & y''' & z''' & 1 \end{bmatrix}^T = \boldsymbol{T}''' \times \boldsymbol{M}'''_\eta \times \boldsymbol{M}'''_\rho \times \boldsymbol{M}'''_\phi \times \begin{bmatrix} u''' & v''' & w''' & 1 \end{bmatrix}^T \quad (7)$$

For the implementation of computer simulation using ray-tracing method, the projections are generated by the intersecting distances which are solved through the equations of the source trajectory function and the geometrical phantom function. For the voxel-driven method, the projections are summed by the weighted voxel values of the phantom in the imaging region.

In the practical application, we utilize the ray- tracing algorithm to implement the computer simulation of CT imaging and adopt the voxel-driven algorithm to implement the computer simulation of pinhole SPECT imaging with collimator detector response blurring[12]. The statistical distribution and noise degrading in the projections are incorporated after the analytical simulation procedure.

3 Simulation results

To validate our developed analytical computer simulation techniques, we made a series of performance evaluation using phantom computer simulations for cone-beam CT, single-pinhole SPECT with adaptive scan modes and multi-pinhole SPECT imaging. Also, we developed several image reconstruction algorithms, which are Feldkamp algorithm[13], 3D pinhole OS-EM algorithm[9,14] with circular and helical scans, and 3D multi-pinhole OS-EM algorithm. These algorithms will be implemented and demonstrated by the experiments

3.1 Cone-beam CT simulation

We first implemented a mathematical 3D Shepp Logan phantom which was often used to evaluate the performance of image reconstruction algorithms in the early CT studies. The phantom is super-positioned by 10 ellipsoids with different densities and sizes. The detail about this phantom is depicted in the reference [2]. Fig.2 shows the trans-axial image of the computerized phantom (Fig.2a), and its 3D perspective rendering (Fig.2b). The noise-free projections were generated with ray tracing method, and acquired with 128128 detector bins and 120 angular views over 360° circular-orbit scan with a magnitude 2.5 of Focal- length/ROR. Fig.2(c) shows a sample projection. No degrading factors such as statistical fluctuation scatter and noise effects were considered in the CT simulation. The data were reconstructed using Feldkamp algorithm. As comparison, Fig.2(d) shows that a reconstruction trans-axial image is the same slice of the phantom in Fig.2(a). We see that the analytical ray-tracing algorithm could provide a flexible and efficient computer simulation for the image reconstruction studies of CT imaging.

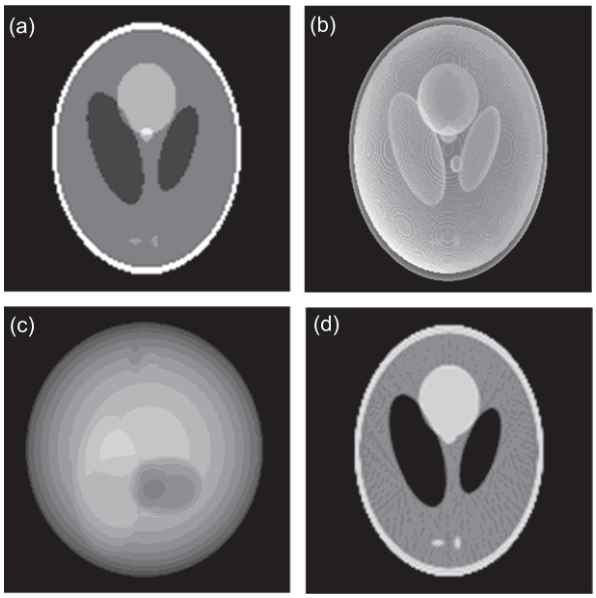

Fig.2 Computation simulation of 3D Shepp-Logan phantom forcone-beam CT imaging. (a) A sample trans-axial slice image of phantom. (b) 3D perspective rending image. (c) A sample projection image by the ray-tracing algorithm. (d) The reconstructed trans-axial image by Feldkamp algorithm.

3.2 Single-pinhole SPECT simulation

To validate the performance of the reconstruction algorithms developed and system designed for pinhole SPECT imaging, a couple of phantom simulations were performed, and used to evaluate the trans-axial reconstructed resolution with circular scan and the axial reconstructed resolution with helical scan. The imaging parameters of the simulations were based on the configuration of our Micro-SPECT system[8].

A mathematical 3D Jaszczak phantom was developed to simulate the pinhole SPECT phantom experiments. Based on the Ultra-Micro Hot Spot Phantom (Data Spectrum, Hillsborough, NC, USA, shown in Fig.3a), the phantom consists of 6 sets of different diameter of hot spot channels: 2.4, 2.0, 1.7, 1.35, 1.0 and 0.75 mm. Fig.3(b) shows a sample projection of the practical phantom imaging experiment by our Micro-SPECT system. We present the 3D perspective rendering of the developed mathematical phantom in Fig.3(c) and its trans-axial image in Fig.3(e). The noise-free projections were generated by voxel-driven algorithm with 1.0 mm keel -edge pinhole collimator, and blurred further with Poisson statistical distribution and noise contaminated, of which a sample projection is shown in Fig.3(d). No scatter and attenuation effects were considered in this simulation. The data were acquired with 70 × 70 detector bins and 90 angular views over 360° circular- orbit scan with 35 mm radius of rotation (ROR). The projection data were reconstructed using 3D pinhole OS-EM algorithm. Fig.3(f) shows the

OS-EM reconstruction image of the simulated projections. As compared with the practical imaging experiments, the analytical simulations have good validity to approach the real imaging system for the reconstruction algorithm study.

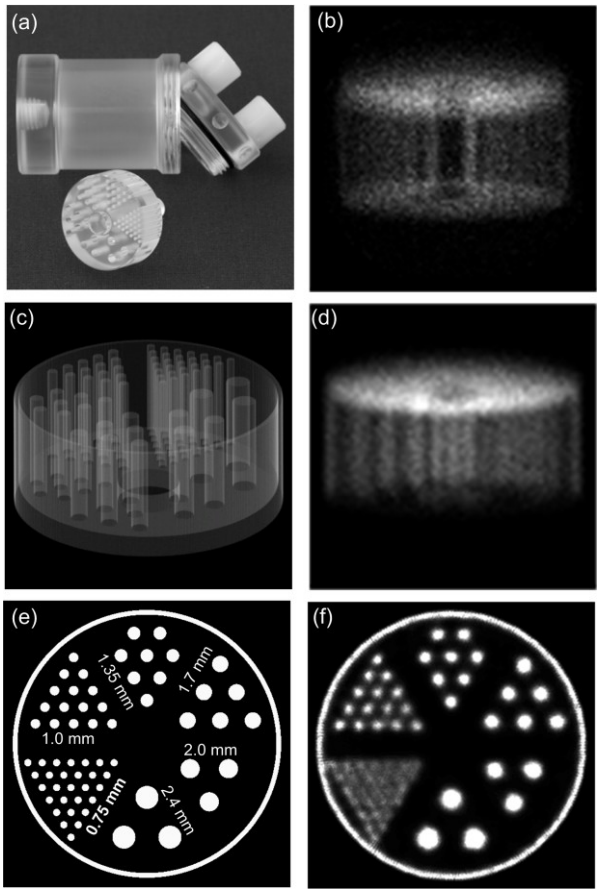

Fig.3 Computation simulation of 3D Hot-Spot phantom for circular single-pinhole SPECT imaging. (a) The Jaszczak phantom. (b) One sample projection image by our Micro-SPECT. (c) 3D perspective rendering of the mathematical phantom. (d) One sample projection image of the computer simulation with keel-edge pinhole collimator response and statistical noise blurring. (e) The trans-axial slice image of the phantom. (f) The reconstructed trans-axial image by 3D pinhole OS-EM algorithm.

Also, we implemented a mathematical 3D Defrise phantom to validate the simulation and reconstruction algorithm for pinhole SPECT with helical scan mode. Based on the Ultra-Micro Defrise Phantom (Data Spectrum, Hillsborough, NC, USA, shown in Fig.4a), the phantom consists of 7 flat uniform cylindrical disks to simulate the interlayer's hot activity solutions. 3D perspective rendering of the mathematical phantom and its central axial slice image are shown in Fig.4(c and e). The noise-free projections were generated by voxel-driven algorithm with 1.0 mm keel-edge pinhole collimator detector response and further with statistical noise blurring. No scatter and attenuation effects were considered in this simulation. The projection data were acquired with 70 × 70 detector bins with 37 mm radius of rotation (ROR) and simulated through 180 angular views over 720° by helical scan with 0.15 mm helical pitch. As comparison, one sample projection of the practical phantom imaging experiment by our Micro-SPECT is shown in Fig.4(b), and one sample projection of the simulation is shown in Fig.6(d). The data were reconstructed using our developed 3D pinhole OS-EM algorithm and the central axial reconstructed image is shown in Fig.4(f). The results demonstrate that our developed simulation technique can provide an efficient tool for the helical reconstruction algorithm implementation which improves the axial spatial resolution of reconstruction image.

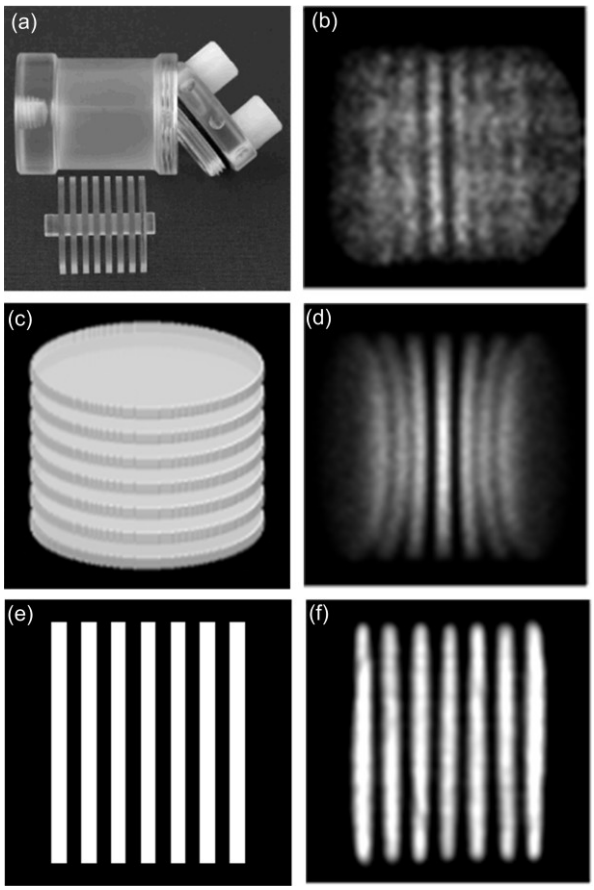

Fig.4 Computation simulation of 3D Defrise phantom for helical single-pinhole SPECT imaging. (a) The practical Defrise phantom. (b) One sample projection image by our Micro- SPECT. (c) 3D perspective rendering of the mathematical phantom. (d) One sample projection image of the computer simulation with keel-edge pinhole collimator response and statistical noise blurring. (e) The central axial slice image of the phantom. (f) The central axial reconstruction image by helical 3D OS-EM algorithm.

3.3 Multi-pinhole SPECT simulation

For multi-pinhole SPECT imaging studies, we further developed analytical multi-pinhole SPECT computer simulation algorithm. To provide sufficient projection sampling, 7 knife-edge pinhole collimators with 0.6 mm aperture diameter are configured at different horizontal and vertical position. The mathematical 3D Hot-Spot and Defrise phantoms in Section 2.2 were used in the multi-pinhole SPECT imaging simulations.

Figure 5(a) shows a sample projection of the simulated 7 pinhole SPECT imaging with 3D Hot-Spot phantom. The noise-free projections were generated with knife-edge pinhole collimator response and Poisson statistical noise blurring without considering any scatter and attenuation effects. The data were acquired with 120 × 120 detector bins and 45 angular views over 360° circular-orbit scan with 35 mm radius of rotation (ROR). The projection data were reconstructed using our developed 3D multi-pinhole pinhole OS-EM algorithm. Fig.5(b) shows the OS-EM reconstruction image of the simulated projections.

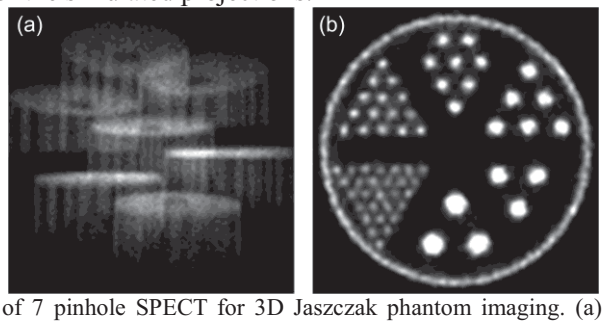

Fig.5 Computational experiment of 7 pinhole SPECT for 3D Jaszczak phantom imaging. (a) A sample projection image of the computer simulation with keel-edge pinhole collimator response and statistical noise blurring. (b) The trans-axial reconstruction image by 3D multi-pinhole OS-EM algorithm.

Figure 6(a) shows a sample projection of the 3D Defrise multi-pinhole SPECT imaging simulation with

noise-free analytical computation with knife-edge pinhole collimator response and statistical blurring. The projection data were simulated with 120 ×120 detector bins with 40 mm radius of rotation (ROR) and by 30 angular views over 360° circular scan. We implemented 3D multi-pinhole OS-EM algorithm to reconstruct the projection data. The central axial reconstructed image is shown in Fig.6(b). The results demonstrate that our developed simulation technique provide an efficient tool for the evaluation of system design and reconstruction algorithms implementation for multi-pinhole SPECT imaging.

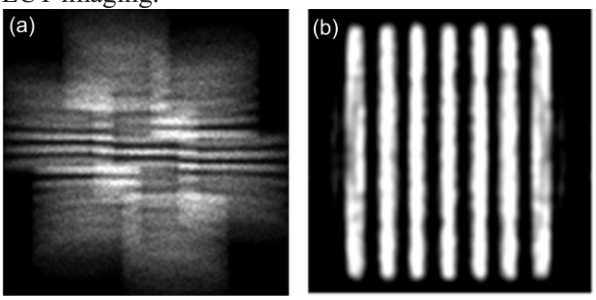

Fig.6 Computational experiment of 7 pinhole SPECT for 3D Defrise phantom imaging. (a) A sample projection image of the computer simulation with keel-edge pinhole collimator response and statistical noise blurring. (b) The central axial reconstruction image by 3D multi-pinhole OS-EM algorithm.

4 Conclusions

We have developed efficient analytical computer simulation techniques for cone-beam CT, single- pinhole SPECT with different scan mode and multi- pinhole SPECT imaging. The performance of the computer simulations were compared to the practical experimental phantom imaging and evaluated using our developed reconstruction algorithms. The results from the simulations and reconstructions of the mathematical phantom imaging show that our developed analytical simulation algorithms with ray-tracing method for cone-beam CT image computation, and voxel-driven method for pinhole SPECT image computation with degrading blurring and adaptive scan modes could provide very good simulated projection data for the evaluation of imaging system and reconstruction algorithms. Our analytical simulation technique is an efficient tool for studying cone-beam CT and pinhole SPECT imaging.

References

[1] Rubinstein R Y, Simulation and the Monte Carlo Method, Wiley-New York, 1981.
[2] Raeside D E, Monte Carlo principles and applications, Phys. Med. Biol. 1976, **21(1):** 181–197.
[3] Zaidi H, Med Phys, 1999, **26(4):** 574-608.
[4] Rogers D W O, Phys Med Biol, 2006, **51(1):** R287–R301.
[5] Herman G T, Fundamentals of Computerized Tomography: Image Reconstruction from Projections, Academic Press, 1980.
[6] Kak A C, Slaney M. Principles of Computerized Tomographic Imaging, IEEE Press, 1988.
[7] Barrett H H, Mayer K J, Foundations of Image Science, Wiley-Interscience, 2003, .
[8] Zhang X Z, Chen F F, Qi Y J, *et al.* Proc IEEE Nucl Sci Symp Conf Rec, 2009, 3318–3321.
[9] Zhang X Z, Qi Y J. Chin Sci Bull, 2011, **56(3):** 340–348.
[10] Zaidi H, Tsui B M W. Proceedings of the IEEE, 2009, **97(12):** 1935–1937.
[11] Yang M, Lang T, Wei Y. Acta Armamentarii, 2006, **27(3):** 437–441.
[12] Zhang X Z, Dai Q S, Qi Y J. Proc IEEE Nucl Sci Symp Conf Rec, 2008, 5255–5259.
[13] Feldkmap L A, Davis L C, Kress J W. J Opt Soc Am Al, 1984, 612–619.
[14] 14 Hudson H M, Larkin R S. IEEE Trans Med Imaging, 1994, **13:** 601–609.